Journal of Low Temperature Physics, Vol. 99, Nos. 3/4, 1995

Magnetism and Transport in the t–t'–J Model

Holger Fehske and Martin Deeg

Physikalisches Institut, Universität Bayreuth, D–95440 Bayreuth, Germany

The normal state properties of high–T_c cuprates are investigated in terms of an extended t–J model using a spin–rotation–invariant slave–boson (SB) technique. A second–neighbour hopping t' of different sign is included to account for band structure effects of both hole– and electron–doped systems. Using the renormalized SB quasiparticle band, the doping and temperature dependence of the Hall resistivity are explored, the results being in accord with experiments on $La_{2-\delta}Sr_\delta CuO_4$ (LSCO), $YBa_2Cu_3O_{6+x}$ (YBCO), and $Nd_{2-\delta}Ce_\delta CuO_4$ (NCCO). The calculated $\vec{q}$–dependence of the dynamical magnetic structure factor $S(\vec{q},\omega)$ shows reasonable agreement with the qualitative features of the neutron scattering cross sections in metallic LSCO– and YBCO–type systems.

PACS numbers: 71.28.+d, 71.45.-d, 71.45.Gm, 72.90.+y, 75.10.-b

The interplay of charge and spin dynamics in the normal phase of high–T_c superconductors holds the key to the understanding of their physics. Therefore, the puzzling normal state behavior of the cuprates, in particular the temperature (T) and doping (δ) dependence of spin susceptibility and Hall resistivity[1–3] or the remarkable differences between LSCO– and YBCO–type spin fluctuation spectra,[4,5] has been under extensive experimental and theoretical study.

To adress these issues from a microscopic point of view, the probably simplest model, describing both strong correlation and band structure effects, seems to be an effective one–band t–t'–J model, in standard notation, given by

$$\mathcal{H}_{t-t'-J} = -t \sum_{\langle i,j\rangle,\sigma} \tilde{c}_{i\sigma}^\dagger \tilde{c}_{j\sigma} - t' \sum_{\langle\langle i,j\rangle\rangle,\sigma} \tilde{c}_{i\sigma}^\dagger \tilde{c}_{j\sigma} + J \sum_{\langle ij\rangle} \left(\vec{S}_i \vec{S}_j - \frac{n_i n_j}{4} \right). \quad (1)$$

$\mathcal{H}_{t-t'-J}$ includes apart from the antiferromagnetic (AFM) exchange interaction J and the NN transfer t, a direct NNN hopping t' on a square lattice. From band–structure theory, a ratio $t'/t = 0 \ldots -0.16$ (-0.4) has been found for the hole–doped LSCO (YBCO) family, where t=0.3–0.4 eV. The case $t' > 0$ corresponds to the electron–doped systems ($\delta < 0$), e.g. NCCO ($t'/t = 0.16$). Note that the t'–term suffices to reproduce the observed Fermi surface geometry (ARPES measurements) for YBCO and NCCO in the noninteracting limit.[6] To compare our theoretical results with experiments, we fix $J/t = 0.4$, and take $t = 0.3$ eV as the energy unit.

For an adequate description of spin and charge degrees of freedom in $\mathcal{H}_{t-t'-J}$, we adopt the $SU(2)\otimes U(1)$ spin–rotation–invariant SB technique[7] within a functional integral approach. At the saddle–point level, we look for an extremum of the bosonized action with respect to SB and Lagrange parameter (λ) fields using the ansatz $\vec{m}_i = m(\cos\vec{Q}\vec{R}_i, \sin\vec{Q}\vec{R}_i, 0)$ for the local magnetization. Thereby, the "order vector" $\vec{Q}$ is introduced to describe para–, ferro–, and antiferromagnetic, as well as incommensurate (1,1)–, (1,0)– and (1,π)–spiral states. Taking into account all these phases, the renormalized quasiparticle band, given by

$$E_{\vec{k}\pm} = \delta(1+\delta)(\varepsilon_{\vec{k}}+\varepsilon_{\vec{k}-\vec{Q}})/y - \tilde{\mu} \pm \left[\delta^2(\varepsilon_{\vec{k}}-\varepsilon_{\vec{k}-\vec{Q}})^2/y + [m\delta(\varepsilon_{\vec{k}}+\varepsilon_{\vec{k}-\vec{Q}})/y+\lambda]^2\right]^{1/2}, \tag{2}$$

has to be determined in a self–consistent way at each doping level δ from the nonlinear stationary equations for m, λ and $\vec{Q}$, where $\tilde{\mu}$ denotes the chemical potential, $\varepsilon_{\vec{k}} = -2t(\cos k_x + \cos k_y) - 4t' \cos k_x \cos k_y$, and $y = (1+\delta)^2 - m^2$.

Fig. 1 (a) displays the variation of the "extremal" wave vector $\vec{Q}$ as a function of doping (included are experiments for LSCO[4] (□)). Obviously, the t'–term provides a possible origin for the experimentally observed asymmetry in the persistence of AFM of hole– and electron–doped systems. Note that our AFM solution is *globally* stable against phase separation near half–filling (for a complete phase diagram see Ref. 8).

In a next step, we calculate the Hall resistivity in the relaxation time approximation by the standard Brillouin zone integrals, where Fermi surface and correlation effects are involved via the SB band (2). In Fig. 1 (b), $R_H(\delta, T)$ is shown for different values of t'/t in comparison to experiments on LSCO[1] (□), NCCO[3] (◇) at 80 K, and YBCO[2] (△) at 100 K, where for the YBCO system we use the relation[8] $\delta = (x-0.2)/2$ between the charge carriers in the CuO_2 layers (δ) and the oxygen content (x). We found that the doping [temperature] dependence of R_H is in excellent quantitative [qualitative] agreement with experiments on both hole– [LSCO] and electron–doped (NCCO) systems, including the sign change as function of δ.

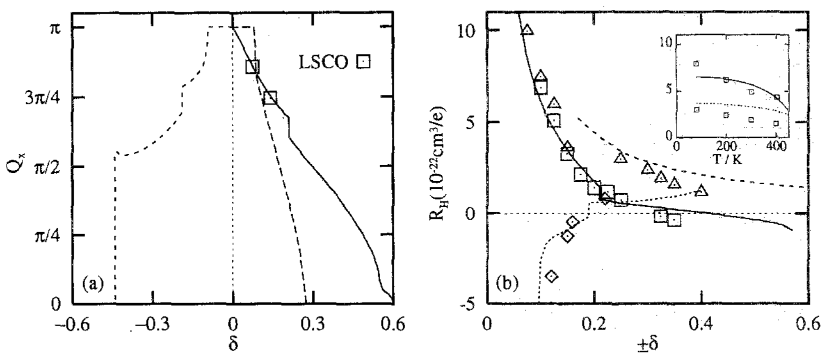

Fig. 1. Spiral wave vector Q_x (**a**) and Hall resistivity R_H (**b**) *vs* δ [T] at $t'/t = 0$ (solid) [inset (**b**): δ=0.1 (solid), 0.15 (dashed)], −0.4 (dashed) and 0.16 (dotted).

For YBCO, the t'–term gives the correct tendency for $R_H(\delta, T)$.

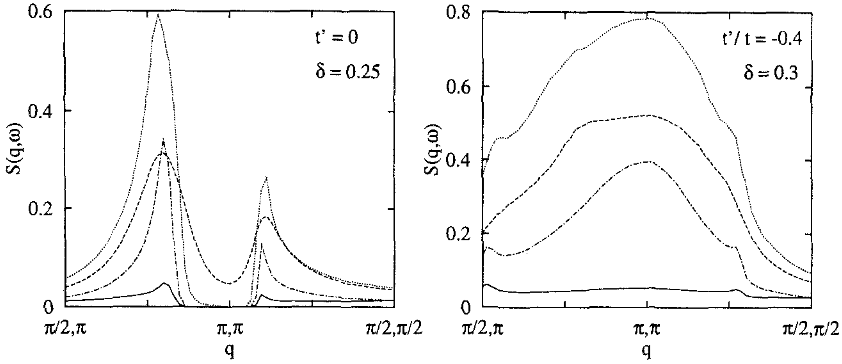

Fig. 2. $S(\vec{q},\omega)$ for J=0.4 at {ω [meV]; T [K]}={10; 35} (chain dotted), {10; 200} (dashed), and {30; 35} (dotted) compared to the case J=0 at {10; 35} (solid).

Finally the spin–excitation spectrum as observed in neutron scattering in LSCO and YBCO is examined in the paraphase on the basis of the RPA dynamical spin structure factor[9]

$$S(\vec{q},\omega) = \frac{1}{\pi}\frac{1}{1-\exp(-\hbar\omega/k_BT)}\,\mathrm{Im}\left\{\frac{\overline{\chi}_o(\vec{q},\omega)}{1+J(\cos q_x+\cos q_y)\,\overline{\chi}_o(\vec{q},\omega)}\right\}, \quad (3)$$

where the irreducible susceptibility $\overline{\chi}_o(\vec{q},\omega)$ contains the (dressed) SB Green propagators. The $\vec{q}$–dependence of $S(\vec{q},\omega)$ along the symmetry axis is shown in Fig. 2 at different ω and T far from the RPA magnetic instability. For LSCO–type parameters we found pronounced incommensurate (IC) peaks[4] with strongly T and ω dependent widths. Here the $\vec{q}$–variation of $S(\vec{q},\omega)$ is mainly governed by that of $\overline{\chi}_o(\vec{q},\omega)$. (Note that while the IC–peak position obtained from the SB IC–vector Q_x can be parametrized consistent with the experimental observation that $Q_x/\pi \simeq (1-2\delta)$ (cf. Fig. 1 (a)), the one–band RPA calculation of $S(\vec{q},\omega)$ yields IC–peaks scaling rather as $Q_x^{RPA}/\pi \simeq (1-\delta)$.) By contrast the same plot for YBCO–type parameters shows a broad, nearly T–independent, maximum around the (π,π) point[5] which, due to the flat topology of $\overline{\chi}_o$, mainly reflects the $\vec{q}$–dependence of $J(\vec{q})$ (see (3)).

REFERENCES

1. H. Tagaki et al., *Phys. Rev. B* **40**, 2254 (1989).
2. E. Jones et al., *Phys. Rev. B* **47**, 8986 (1993).
3. H. Tagaki, S. Uchida and Y. Tokura, *Phys. Rev. Lett* **62**, 1197 (1992).
4. S.-W. Cheong et al., *Phys. Rev. Lett.* **67** 1791 (1991).
5. J. Rossat–Mignod et al., *Physica C* **185–189**, 86 (1991).
6. T. Tohyama and S. Maekawa, *Phys. Rev. B* **49**, 3596 (1994).
7. M. Deeg, H. Fehske and H. Büttner, *Europhys. Lett.* **26**, 109 (1994).
8. M. Deeg and H. Fehske, *Phys. Rev. B*, in press, (1994).
9. A similar approach can be found in H. Kohno, T. Tanamoto and H. Fukuyama, *Physica B* **186–188**, 941 (1993), Q. Si et al., *Phys. Rev. B* **47**, 9055 (1993) and M. Lavagna and G. Stemmann, *Phys. Rev. B* **49**, 4235 (1994).